Original Paper

Ex vivo MRI facilitates localization of cerebral microbleeds of different ages during neuropathology assessment

Sukriti Nag[1,2], Er-Yun Chen[2], Ryan Johnson[2], Ashish Tamhane[2], Konstantinos Arfanakis[2,3], Julie A. Schneider[1,2,4]

[1] *Department of Pathology (Neuropathology), Rush University Medical Center, Chicago, IL, USA*

[2] *Rush Alzheimer's Disease Center, Rush University Medical Center, Chicago, IL, USA*

[3] *Department of Biomedical Engineering, Illinois Institute of Technology, Chicago, IL, USA*

[4] *Department of Neurological Sciences, Rush University Medical Center, Chicago, IL, USA*

Corresponding author:
Sukriti Nag · Rush Alzheimer Disease Center · Suite 1000 · Rush University Medical Center · 1750 W Harrison Street · Chicago, IL 60612 · USA
Sukriti_Nag@rush.edu

Submitted: 20 October 2021 · Accepted: 12 December 2021 · Copyedited by: Christian Thomas · Published: 20 December 2021

Abstract

Cerebral microbleeds (CMBs) identified by in vivo magnetic resonance imaging (MRI) of brains of older persons may have clinical relevance due to their association with cognitive impairment and other adverse neurologic outcomes, but are often not detected in routine neuropathology evaluations. In this study, the utility of ex vivo MRI in the neuropathological identification, localization, and frequency of CMBs was investigated. The study included 3 community dwelling elders with Alzheimer's dementia, and mild to severe small vessel disease (SVD). Ex vivo MRI was performed on the fixed hemisphere to identify CMBs, blinded to the neuropathology diagnoses. The hemibrains were then sliced at 1 cm intervals and 2, 1 or 0 microhemorrhages (MH) were detected on the cut surfaces of brain slabs using the routine neuropathology protocol. Ex vivo imaging detected 15, 14 and 9 possible CMBs in cases 1, 2 and 3, respectively. To obtain histological confirmation of the CMBs detected by ex vivo MRI, the 1 cm brain slabs were dissected further and MHs or areas corresponding to the CMBs detected by ex vivo MRI were blocked and serially sectioned at 6 µm intervals. Macroscopic examination followed by microscopy post ex vivo MRI resulted in detection of 35 MHs and therefore, about 12 times as many MHs were detected compared to routine neuropathology assessment without ex vivo MRI. While microscopy identified previously unrecognized chronic MHs, it also showed that MHs were acute or subacute and therefore may represent peri-mortem events. Ex vivo MRI detected CMBs not otherwise identified on routine neuropathological examination of brains of older persons and histologic evaluation of the CMBs is necessary to determine the age and clinical relevance of each hemorrhage.

Keywords: Alzheimer's dementia, Cerebral microbleeds, Ex vivo magnetic resonance imaging, Hemosiderin, Microhemorrhages

Introduction

Cerebral microbleeds (CMBs) are defined as rounded or ovoid, hypointense foci that are best demonstrated in susceptibility-weighted and gradient echo magnetic resonance imaging (MRI). In most studies, the upper limit of the diameter of CMBs is 5-5.7 mm [1-3], although a diameter of 10 mm has also been reported [4]. Neuroimaging studies show that CMBs tend to increase with age being observed in 5% of healthy adults [5, 6], and 7% of volunteers having a mean age of 62.1 ±7.4 years who were enrolled in the UK Biobank study [7]. CMBs are reported in 18% of subjects between 60 to 69 years, while in those older than 80 years prevalence increases to 38% [6]. CMBs have also been associated with increased risk of stroke in the general population [8]. Prevalence is higher in those with ischemic stroke and with non-traumatic intracerebral hemorrhage, being 34% and 60%, respectively [5]. In the latter study, CMBs were associated with hypertension or diabetes mellitus in otherwise healthy adults, while in adults with cerebrovascular disease they were only associated with hypertension. The frequency of CMBs is 84.9% in those with subcortical vascular dementia and in these subjects CMBs were related to cognitive impairment in multiple domains [9].

In most studies, CMBs were identified by in vivo MRI alone [8-12], while in a few studies by neuropathology assessment alone in which they are referred to as microhemorrhages (MHs) [13]. The development of ex vivo MRI led to studies correlating ex vivo MRI findings with neuropathology in selected brain slabs [1, 2, 14-16]. In these studies, CMBs were considered to be markers of focal hemosiderin deposition that remained in macrophages for years following a MH [1, 11]. There is increasing evidence that the pathologic correlate of CMBs is more varied than just MHs since a significant association was observed between hemosiderin collections in the putamen and indices of small vessel ischemia such as microinfarcts, arteriolosclerosis and lacunes in any of the brain regions examined [2, 14].

The aim of the present study was to characterize the morphologic correlate of CMBs identified by ex vivo MRI of a single cerebral hemisphere of 3 brains with and without MHs identified on initial neuropathology assessment. This was followed by detailed neuropathology assessment to determine the spectrum of pathology associated with the CMBs identified by ex vivo MRI. Since one in five patients with Alzheimer's disease (AD) has CMBs [17], and the frequency of CMBs is higher in association with cerebral amyloid angiopathy (CAA) [2, 18], and arteriolosclerosis [1, 19], 3 community dwelling elders with a clinical diagnosis of Alzheimer's dementia and varying degrees of small vessel disease (SVD) were selected for assessment.

Materials and methods

The criteria for selection of the three autopsied cases for this study include a clinical diagnosis of Alzheimer's dementia and pathologic evidence of CAA and arteriolosclerosis as well as absence of a clinical history of traumatic brain injury with loss of consciousness since diffuse axonal injury following head trauma is another potential secondary cause of CMB [11]. Cases were from the Memory and Aging Project (MAP), a large clinical-pathology study of aging and dementia with community dwelling participants. The protocols used in this study were approved by the Institutional Review Board of Rush University Medical Center. A signed informed consent was obtained from each participant for an annual clinical evaluation and for brain donation. Participants underwent uniform clinical evaluations at baseline and annually thereafter for odor testing, parkinsonism signs and cognitive function as described previously [20].

Ex vivo imaging

Following removal, the brain was hemisected and one hemisphere with visible gross pathology or one hemisphere with absence of pathology was selected arbitrarily and submerged medial side up in 4 % paraformaldehyde in a container which was rocked back and forth until no more air bubbles escaped from the lateral ventricles. The hemisphere was then placed medial side down and refrigerated. MRI was done on average 1 month postmortem on hemibrains returned to room temperature, immersed in 10% formalin and held in place in a container using a plastic divider. Ex vivo MRI was done using a Siemens 3Tesla MRI scanner and a three-

Table 1: Clinical and pathological findings in 3 cases with a clinical diagnosis of Alzheimer's dementia.

	Case 1	**Case 2**	**Case 3**
Age, years	91.4	96.2	79.2
Sex	Female	Female	Male
Education, years	16	12	16
Blood pressure, mm Hg (last valid)	96/54[a]	171/96[b]	M
MMSE score (last valid)	11[a]	5[b]	9[c]
Total CMBs detected by ex vivo MRI	15	14	9
Post mortem interval, hours	22	8	6
Pathological Diagnoses from blocks taken routinely			
Alzheimer's Disease	-	+	+
CERAD	Probable	Probable	Definite
Braak stage	I	III	IV
Thal stage	3	3	5
ADNC	Low	Inter-mediate	Inter-mediate
Hippocampal Sclerosis	+	-	-
LATE-NC - Stage	3	3	0
Cerebral amyloid angi-opathy, mild-severe	Mild	Mild	Severe
Arteriolosclerosis	Mild	Mod-Severe	Mild
Atherosclerosis	Possible	Mild	Mild-Mod
Macroscopic infarcts, chronic	-	4	1
Microscopic infarcts, chronic	-	7	1
Total MHs using the routine protocol (no ex vivo MRI)	2	1	0
Total MHs post ex vivo MRI			
Acute	5	2	5
Subacute	9	0	0
Chronic	1	12	1
Additional pathologies in blocks taken post ex vivo MRI			
Microinfarct, chronic	-	1	1
Microinfarct, subacute	0	1	0

Abbreviations: **ADNC -** Alzheimer's disease neuropathologic change; **CERAD -** Consortium to establish a registry for Alzheimer's disease; **CMBs -** cerebral microbleeds; **LATE-NC -** limbic predominant age-related TDP-43 neuropathologic change; **M -** missing; **MHs -** microhemorrhages; **Mod -** moderate.
Values obtained 3[a], 7[b] and 4[c] months prior to death.

dimensional multi-echo gradient echo (GRE) sequence with 6 echoes (TE = 5 + n×5 ms (n=0-5), TR = 35 ms), an acquired voxel-size of 1×1×1 mm^3, and a scan time of about 8 min. Microbleeds were identified by a trained reader who was blinded to clinical and pathology data. CMBs were diagnosed when a relatively round, small, hypointense region of few mm in diameter was observed on the last echo of the GRE data. At least half of the hypointensity had to be surrounded by brain parenchyma to qualify. Elongated, vessel-like hypointensities and potential mimics, including lesions in the subarachnoid space, calcifications, or vascular malformations were excluded.

Neuropathology assessment

The mean postmortem interval for cases 1-3 was 22, 8 and 6 hours, respectively (**Table 1**). A standard protocol was used to evaluate brains which included cutting each hemibrain into 1 cm coronal slabs guided by a plexiglass jig and brain blocks from eleven brain regions and any MH noted on the cut surfaces of the slabs were blocked for microscopy as described previously [21]. Pathological diagnosis of AD, hippocampal sclerosis (HS), limbic predominant age-related TDP-43 encephalopathy neuropathologic change (LATE-NC), macroscopic and microscopic infarcts were made as described previously [21]. CAA was assessed in meningeal and intracortical vessels in sections from the midfrontal, midtemporal, inferior parietal and occipital cortices which were immunostained for β-amyloid and graded as described previously [22]. Arteriolosclerosis was assessed in the basal ganglia and graded using a semi-quantitative scale from 0 (none) to 6 (severe) as described previously [21].

Microhemorrhages

The ex vivo MRI images were superimposed on photomicrographs of the brain slabs to identify the region of the suspected CMB. In this protocol, each 1 cm slab was further dissected to detect the CMBs observed in the ex vivo MR images and brain blocks containing these CMBs were obtained. In instances where a MH was not identified on the cut surface of the brain slab, a block was obtained in the region containing the CMB identified by ex vivo MRI. All brain blocks were processed using standard techniques and embedded in paraffin. Each block was serially sectioned at 6µm thickness to obtain 200-250 serial sections from each block. Every 10th section was stained with hematoxylin and eosin (HE) and

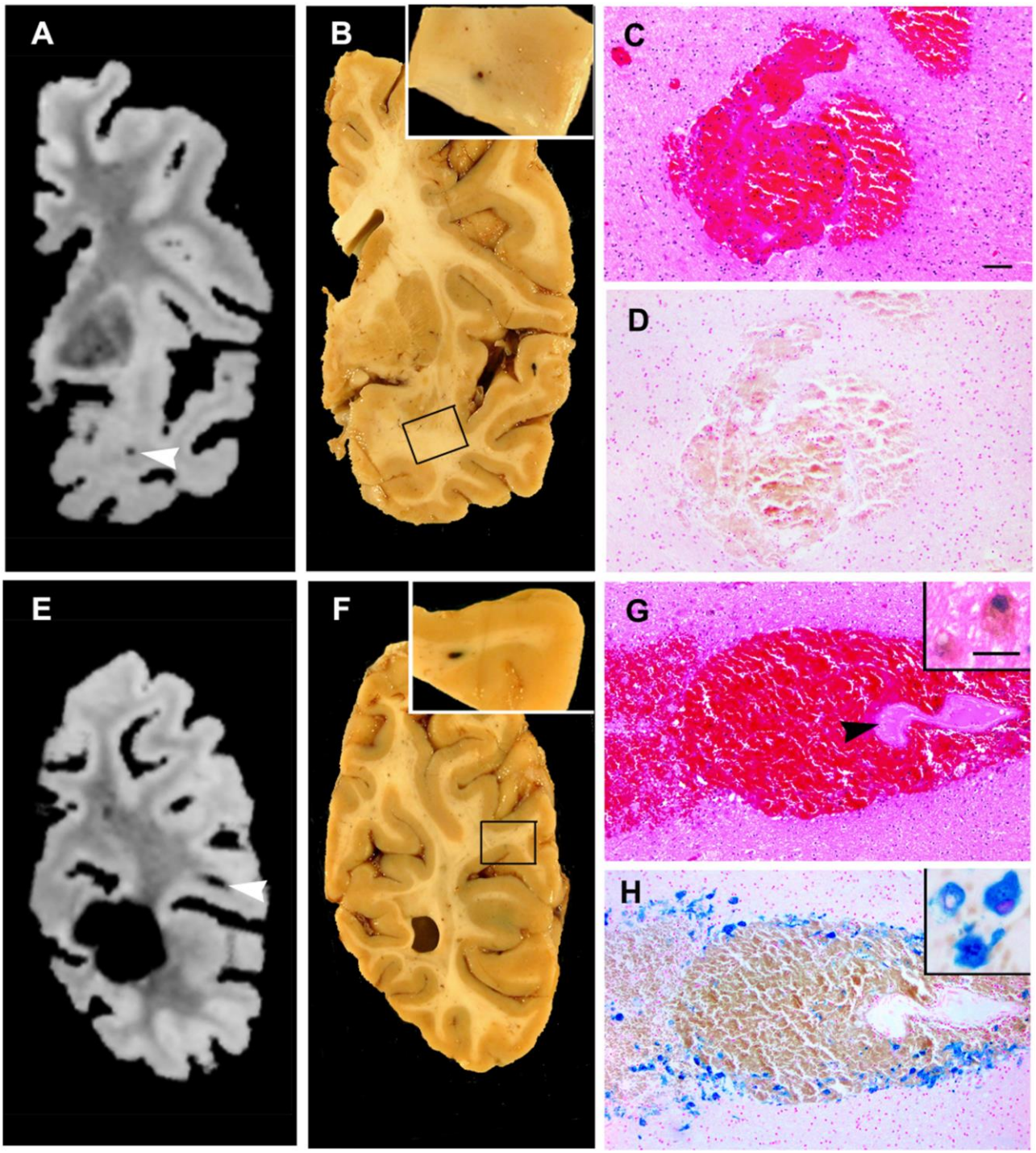

Figure 1: Ex vivo MRI scans, corresponding brain slabs and microscopy of acute and subacute hemorrhages are shown. **(A)** The MRI scan shows a CMB in the white matter of the temporal lobe (arrowhead). **(B)** The corresponding brain slab was further sliced in the area of the CMB shown in the ex vivo MR scan and delineated by the rectangle to detect the MH which is shown in the inset (case 1, MH#6). **(A, B)** Also present is another CMB at the interface of the cortex and white matter of the superior temporal gyrus (case 1, MH#8). **(C)** Microscopy of a hematoxylin and eosin (HE) stained section from MH#6 shows an acute hemorrhage with extravasation of red blood cells through a venular wall into the surrounding brain. **(D)** This MH shows no macrophages or hemosiderin by the Perl's Prussian blue stain at this level or in serial sections. **(E)** Ex vivo MRI shows a CMB in the white matter of the inferior parietal lobule (arrowhead). **(F)** Further slices of the corresponding brain slab in the area delineated by a rectangle shows a MH (case1, MH#14) in the white matter which is shown in the inset. **(G)** An HE stained section of the MH shows significant extravasation of red blood cells through an arteriolar wall (arrowhead) into the neuropil. A few pigment-laden macrophages are identified at the periphery of the hemorrhage (inset). **(H)** The increased number of macrophages are clearly evident by the Perl's Prussian blue stain. Higher magnification of the hemosiderin positive macrophages is shown in the inset. **C**, **D**, **G**, **H** scale bar = 50 µm; insets G, H scale bar = 10 µm

the adjacent section was stained by the Perl's Prussian blue stain for hemosiderin. In select cases, additional sections were stained by HE and for hemosiderin. Immunohistochemistry to detect β-amyloid was done in all CMB's as described previously [22]. The size of MHs was measured using a 1 mm graticule at a magnification of x100.

Results

The age of the three decedents was 91.4, 96.2 and 79.2 years and in keeping with the clinical diagnosis of Alzheimer's dementia, all cases had a low Mini-Mental State Examination score which varied from 5-11 (**Table 1**). Blood pressure data was only available for 2 cases and only case 2 was hypertensive. On routine neuropathology assessment, (**Table 1**) two of the three cases had intermediate likelihood of AD by the NIA-Reagan and ADNC criteria while the third case with low likelihood of AD had hippocampal sclerosis with LATE-NC (stage 3) implying involvement of the amygdala, limbic and neocortical areas by TDP-43 neuronal and glial cytoplasmic inclusions. Regarding vascular changes, cases 1 and 2 had mild CAA while case 3 had severe CAA. Arteriolosclerosis was mild in cases 1 and 3 and moderate-severe in case 2.

Ex vivo imaging detected 15,14 and 9 possible CMBs in cases 1, 2 and 3, respectively (**Table 1**). MR images showed hypointense, rounded areas in the gray or white matter which were interpreted as CMBs. (**Fig. 1A**, **E**, **2A**) The diameter of CMBs measured in the same echo as used for their visualization, varied from 1.56 – 4.20 mm. Most of the CMBs observed in this study were located in the subcortical white matter near the grey/white junction of the frontal, temporal or occipital lobes, although, involvement of gray matter structures such as the midtemporal cortex, thalamus and caudate nucleus were also noted.

Macroscopic findings

The appearance of the MHs on macroscopic examination of the cut surfaces of brain slabs whether using the routine or the extended protocol was similar. MHs appeared as rounded, reddish areas, 1-2 mm in diameter resembling the MH shown in the inset of **Fig. 1B**. In a few cases, there was a focal area of bluish discoloration suggesting presence of a hemorrhage below the cut surface of the brain slab while in other cases no hemorrhage was noted on the cut surface of the slab and was only identified following serial sectioning in the regions showing CMBs by ex vivo imaging (**Fig. 1F**).

Microscopic findings

A total of 12 acute, 9 subacute and 14 MHs were identified by microscopy of the 3 cases which include the 3 MHs observed using routine neuropathology assessment. Most of the hemorrhages (74%) were located in the white matter while the remainder were in grey matter structures such as one in the midtemporal cortex, one in the caudate nucleus and others in the thalamus (**Table 2**). Microscopy of all 35 MHs showed that their diameter varied from 0.2-0.8 mm. Most MHs were associated with arterioles. Among the acute hemorrhages, 3 were associated with venules and 1 with multiple capillaries. In the case of chronic hemorrhages, only one was associated with a venule, while another chronic hemorrhage was associated with both an arteriole and venule which were adjacent to each other, while others were associated with arterioles. On serial sectioning, MHs involved variable lengths of the vessel with some MHs involving short 125-300 µm segments of arterioles while others involved long segments of arterioles varying from 480-780 µm in length. There was no evidence of calcification or vascular malformations, such as a cavernous hemangioma in any of the sections examined. Most blocks showed a single MH correlating with the CMB seen on ex vivo MRI, however, there were 3 instances when the block showed additional MHs which were not identified by ex vivo MRI (**Table 2**).

MHs were acute, subacute or chronic based on the cellular response present. Acute MHs showed extravasation of erythrocytes through the walls of mainly arterioles and fewer venules and extended into the surrounding neuropil (**Fig. 1C**). Serial sectioning of the entire block did not show inflammatory cells or hemosiderin either on HE or the Perl's Prussian blue stain thus their age was not altered (**Fig. 1D**). An additional finding in subacute MHs was the extension of red blood cells further from vessel walls than observed in the acute hemorrhages (**Fig. 1G**). A few intravascular and a variable number of

Table 2: Location and age of microhemorrhages (MH) detected without MRI and pathological features of those detected following ex vivo MRI.

	MH diagnosis by routine NP	**CMBs diagnosed following ex vivo MRI**	**Microhemorrhages (MH) Histological findings**			**Other microscopic findings**
	Location, Age	**Location**	**Age**	**Perl's**	**No. of MHs**	
Case 1						
1		Superior frontal, WM	Acute	-	1	
2		Subcortical WM, between superior and middle frontal gyri	Acute	-	1	
3		Inferior frontal gyrus, WM	Subacute	+	1	
4		Anterior temporal tip, WM	Subacute	+	1	
5		Midtemporal gyrus, WM	Subacute	+	2	
6		Midtemporal gyrus, WM	Acute	-	1	
7	Superior temporal gyrus WM, acute	Superior temporal gyrus, WM	Subacute	+	1	
8		Superior temporal gyrus, WM	Subacute	+	1	
9		Superior temporal gyrus, WM	Subacute	+	1	
10		Postcentral gyrus, WM	Subacute	+	1	
11	Inferior temporal gyrus WM, acute	Inferior temp gyrus, WM	Acute	-	1	
12		Temporal periventricular WM	No MH	-	0	
13		Superior parietal lobule, WM	Acute	-	1	
14		Inferior parietal lobule, WM	Subacute	+	1	
15		Anterior insula, WM	Chronic	+	1	
Case 2						
1		Occipital WM, posterior	No MH	-	0	Dilated vein with luminal blood
2		Occipital WM, anterior	Chronic	+	1	
3	Midtemporal cortex, chronic	Midtemporal cortex	Chronic	+	1	
4		Thalamus, (ventral posterior lateral nucleus)	No MH	-	0	
5		Thalamus, (lateral, posterior nucleus)	Chronic	+	2	Subacute microinfarct-1
6		Thalamus (dorsomedial nucleus)	No MH	-	0	
7		Thalamus (dorsomedial nucleus near midline)	No MH	-	0	Dilated vessels with luminal blood
8		WM near ventro-lateral nucleus of thalamus	Chronic	+	2	
9		Thalamus (ventro-lateral nucleus)	Chronic	+	4	
10		Thalamus (ventro-lateral nucleus)	Chronic	-	1	Chronic microinfarct-1
11		WM ventral to putamen (posterior)	No MH	-	0	
12		WM adjacent to lateral putamen	Chronic	+	1	Perivascular hemosiderin
13		WM ventral to Putamen (anterior)	Acute	-	1	
14		Caudate nucleus	Acute	-	1	

Case 3						
1	No CMB diagnosed	Superior frontal gyrus	No MH	-	0	
2		WM lateral to Putamen	No MH	-	0	Dilated vessels with luminal blood
3		Frontal lobe WM	Acute	-	1	
4		Parietal lobe WM	Acute	-	1	
5		Occipitotemporal gyrus,WM	Acute	-	1	
6		Occipitotemporal gyrus, WM	Acute	-	1	
7		Occipital lobe WM	Acute	-	1	
8		Occipital lobe WM	No MH	-	0	
9		Occipital lobe WM	Chronic	+	1	Chronic microinfarct-1

Abbreviations: **CMBs -** cerebral microbleeds; **MHs -** microhemorrhages; **WM -** white matter.

perivascular macrophages were present and many contained faint brown hemosiderin pigment. The adjacent Perl's-stained section accentuated the macrophage numbers and their hemosiderin content (**Fig. 1H**). The neuropil surrounding the hemorrhage showed vacuolation and sparse gemistocytes. In chronic MHs, a cavity was present containing or surrounded by a variable number of macrophages which showed intense brown cytoplasmic staining due to hemosiderin (**Fig. 2C, D**). The neuropil surrounding the hemorrhage showed fibrillary astrocytes. Adjacent arterioles showed acellular mural thickening with absence of smooth muscle cells and failed to show β-amyloid positivity (**Fig. 2E**). In all MHs, vessels failed to show mural β-amyloid positivity with the exception of one chronic MH (case 2, MH #3) in the midtemporal cortex which showed a disrupted vessel associated with hemosiderin-laden macrophages (**Fig. 2F**) and focal β-amyloid positivity at the periphery of the vessel (**Fig. 2G**). Another pattern of chronic MH was the presence of scattered hemosiderin-laden macrophages in a focal area of the white matter (**Fig. 3A**). Serial sectioning showed that these areas extended for depths of 120-180 µm and were related to terminal arterioles and capillaries (**Fig. 3B**). In some MHs, arterioles with sclerosed, hyaline walls and collapsed lumina were present surrounded by variable numbers of hemosiderin containing macrophages in the neuropil. In one instance, only perivascular collections of few macrophages were present in multifocal areas of the putamen.

In addition to the MHs which correlated with the hypointense areas detected by ex vivo MRI, serial sectioning showed MHs measuring < 0.4 mm in their greatest dimension (**Fig. 3C, D**). These MHs were much smaller than the CMBs identified by ex vivo MRI and were present in 1-3 consecutive sections per block. These small MHs were not included in the total MH counts shown in **Table 1**, since they did not correlate with any of the reported hypointensities observed by MRI and since they were too small to be visualized by a 3T scanner.

Although 38 CMBs were described in the ex vivo MR scans, in 8 instances microscopy did not show MHs despite additional slicing of brain slabs and microscopy of serially sectioned blocks. On microscopy, 3 of these presumed CMBs showed 2-3 large dilated vessels with luminal blood (**Table 2**). In 2 presumed CMBs, the area of hypointensity represented the site of entry of penetrating arterioles in the lateral and inferior portion of the putamen and in 2 presumed CMBs the area of hypointensity probably represented the depths of sulci and only in one case no pathology was detected. Additional pathology identified by serial sectioning were chronic microinfarcts in 2 cases and a subacute microinfarct in 1 case (**Table 2**) and microinfarcts measuring < 0.4 mm in their greatest dimension (**Fig. 3E, F**).

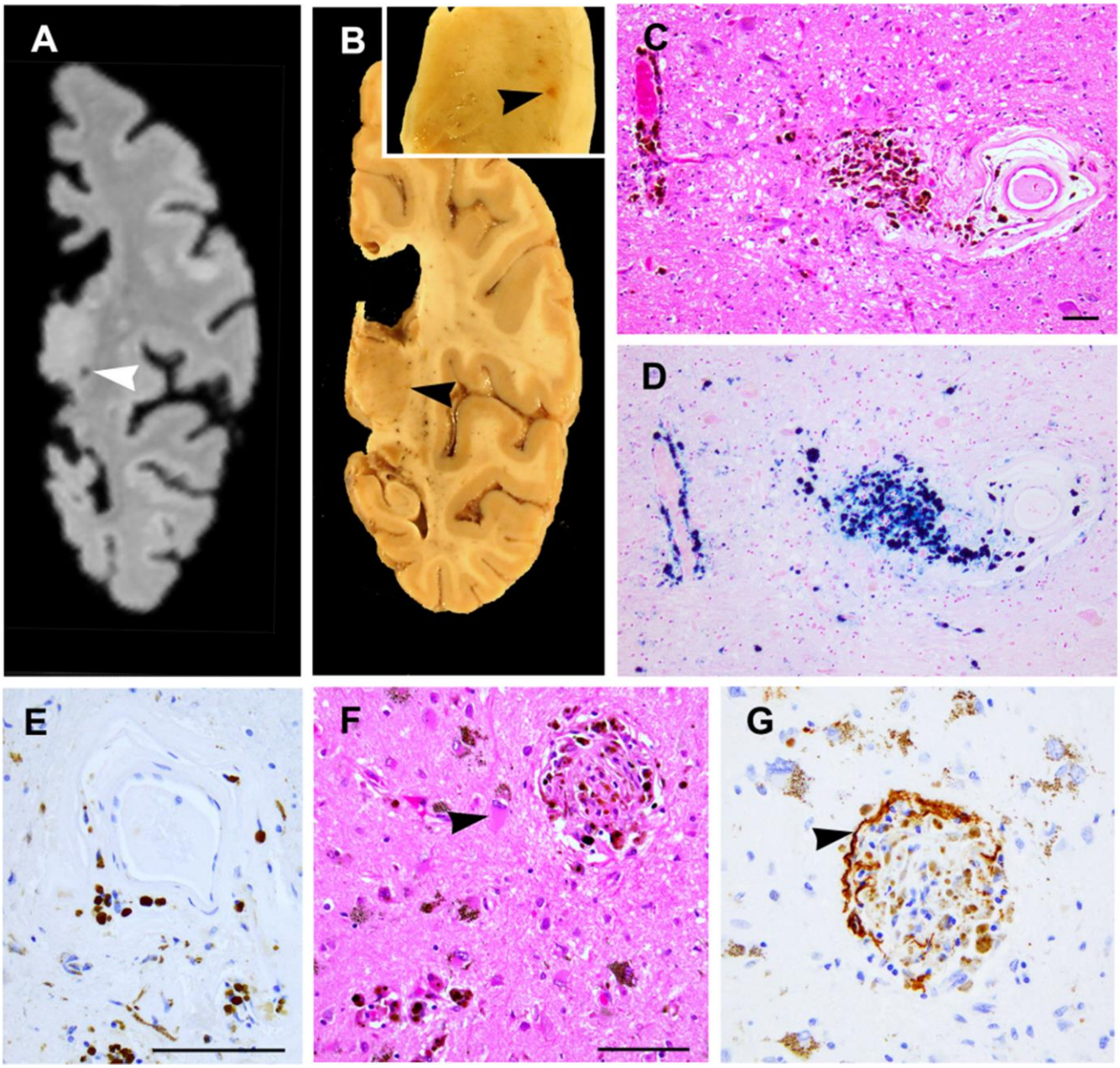

Figure 2: Ex vivo MRI scan, corresponding brain slab and microscopy of chronic grey matter hemorrhages are shown. **(A)** Ex vivo MRI shows a CMB in the lateral thalamus. **(B)** The corresponding brain slab shows an area of reddish discoloration (arrowhead) which is shown at higher magnification in the inset (case 2 MH#8). **(C)** The corresponding HE stained section shows a cavity containing hemosiderin-laden macrophages adjacent to an arteriole which shows focal mural disruption and double-barreling. A nearby arteriole shows perivascular hemosiderin-laden macrophages. **(D)** The adjacent section shows strong Prussian blue staining of the hemosiderin collections. **(E)** Immunostaining of the arteriole shown in C and D fails to show mural β-amyloid although the double barreling is highly suggestive of CAA. **(F)** A focal hemorrhage in layer three of the superior temporal cortex shows disruption of a vessel associated with hemosiderin-laden macrophages which are also present in the surrounding neuropil along with gemistocytes (arrowhead) **(G)** The adjacent section shows focal β-amyloid immunostaining at the periphery of the vessel (arrowhead). **C**, **D** scale bar = 50 µm; **E**, **G** scale bar = 50 µm, **F** scale bar = 50 µm.

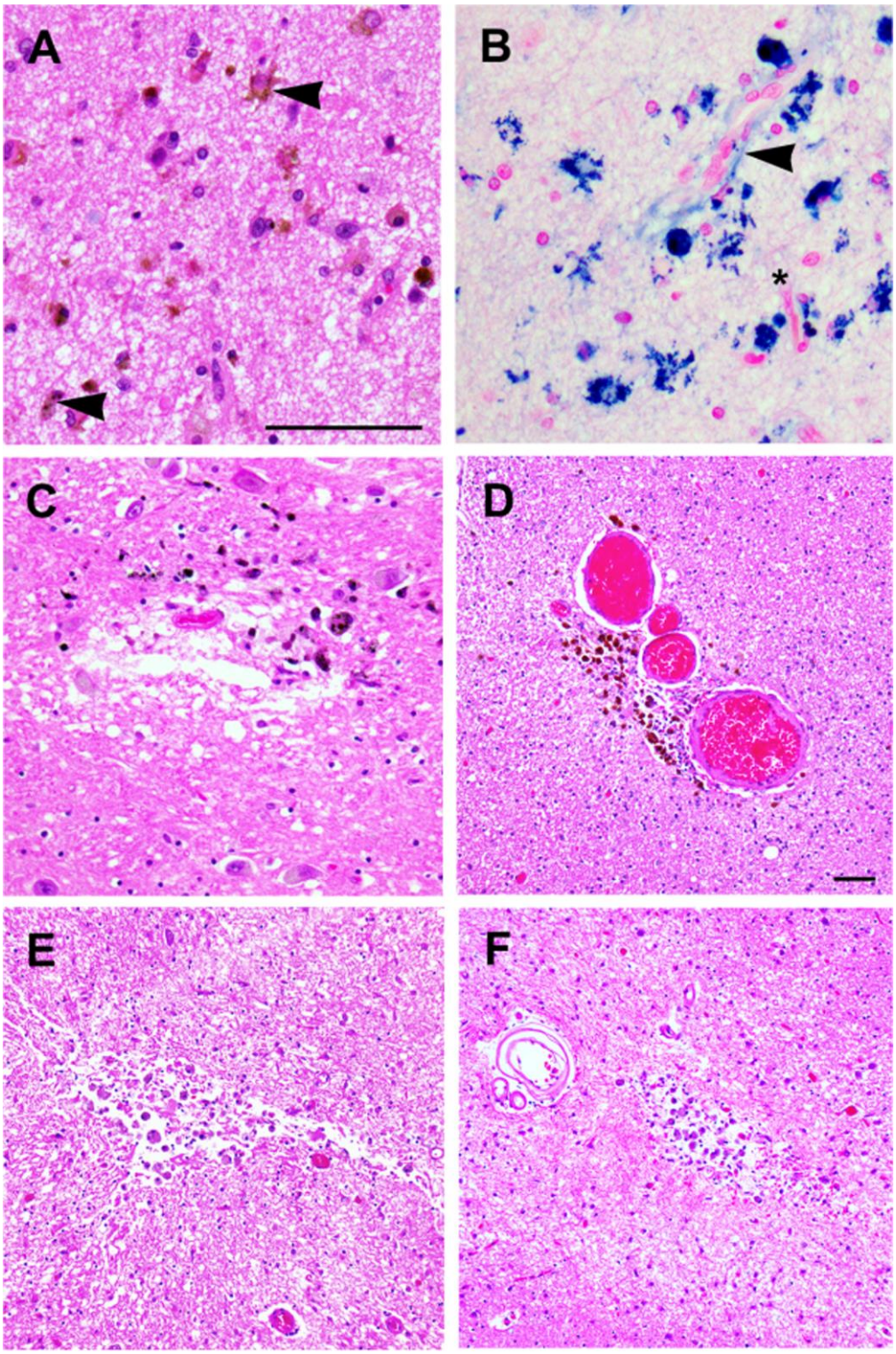

Figure 3: Microscopy of chronic hemorrhages and chronic microinfarcts. **(A)** An example of a focal chronic white matter hemorrhage (600 x 300 µm) showing scattered hemosiderin-laden macrophages (arrowheads). **(B)** The adjacent section shows a terminal arteriole (arrowhead) and capillary (below the asterisk) with all macrophages showing positivity by the Perls's Prussian blue stain. Serial sections show two small MHs **(C, D)** measuring 200 **(C)** and 300 **(D)** µm in their longest dimension and two chronic microinfarcts **(E, F)** measuring 300 **(E)** and 200 **(F)** µm which do not correlate with any CMBs observed in the ex vivo scans. The microinfarcts show disruption of the neuropil and many macrophages some of which appeared pale brown suggesting hemosiderin but were negative by the Perl's Prussian blue stain. **A-C** scale bar = 50 µm; **D-F** scale bar = 50 µm.

Discussion

This study demonstrates the utility of ex vivo MRI in the identification of MHs by neuropathology assessment. Routine macroscopic assessment showed a total of 3 MHs while both macroscopic and microscopic assessment after ex vivo MRI showed about 12 times as many MHs. In cases 1 and 2, the number of MHs was increased from that seen on routine neuropathology assessment, while in case 3, no MHs were identified on routine neuropathology assessment but were detected by ex vivo MRI followed by neuropathology assessment. Thus, routine neuropathology assessment alone is unreliable in detecting the presence or the total number of MHs in a specific brain.

The MHs identified in this study by microscopy were smaller than indicated by their MR appearance being < 1 mm in diameter. The finding that CMBs detected by MRI appear larger on gradient-echo sequences compared with the actual tissue lesions is attributed to the "blooming effect" of the MR signal at the border of these lesions [11, 23]. Also, further shrinkage of brain blocks during the processing schedule for paraffin embedding may contribute to the reduced diameter observed on microscopy. Diameters measured in ex vivo scans were reported to be on average 1.6 ±0.75 times [2] or 4 times [16] higher than the diameter identified by pathology assessment. However, since the size of a CMB on MRI depends on imaging parameters, such as field strength and pulse sequence, comparison of CMB size across studies is probably not valid due to the difficulty in implementing identical imaging parameters on different MRI systems [11]. The localization of MHs in the current study in both the grey and the subcortical white matter near the grey/white junction is similar to previous observations [1, 2, 13]. In addition, involvement of mainly arterioles and fewer capillaries and intracerebral venules in MHs has also been reported in a prior study [13]. In the current study, 38 blocks were examined by serial sectioning and 35 MHs were identified in the 3 cases with some blocks having more MHs than identified by ex vivo MRI. The very small MHs observed only by histology and not by ex vivo MRI in the present and previous studies [1, 13], are probably beyond the sensitivity of a 3T MRI scanner. Ex vivo imaging using a 7T scanner and high resolution (200 um isotropic resolution) can detect 2.6 times as many CMBs as compared to an in vivo 7T MRI scanner while ultrahigh resolution detects additional hypointensities which on microscopy show vessel pathology but no additional hemorrhages [16].

The criteria used in the current study for aging MHs as acute, subacute or chronic is supported by previous experimental studies of rodent [24, 25] and rabbit [26] brains with MHs in which the time course of the cellular reactions was documented. During the acute phase up to 48 hours, the hematoma is surrounded by edematous neuropil and no inflammatory cells. The initial peri-hemorrhage inflammatory response at 48 hours consists of few blood-borne neutrophils and brain-resident microglia (CX3CR1 positive) which migrate to the lesion site from the surrounding tissue. Astrocytic activation is reported to occur a few days after the onset of the microglial response. Conversion to hemosiderin begins at day 5 after the injection of either blood or red blood cells into brain [26]. By day 8, macrophages (brain-resident microglia and fewer blood-derived macrophages) are abundant and show evidence of proliferation at the lesion site. By 2 weeks, the inflammatory response resolves. Therefore, subacute MHs are up to 2 weeks or few weeks of age. Changes between few weeks and 3 months are not reported, however, at 3 months cavities are observed at the MH site with variable numbers of macrophages showing abundant hemosiderin. Fibrillary gliosis is present and arterioles in the area showed mural thickening which is not related to amyloid as noted in the current and a previous study [13], while in another study mural β-amyloid was detected in a bleeding vessel [2]. Therefore, chronic MHs are 3 months of age or older.

The frequency of acute MHs in the current study was 34%, while other studies have reported percentages of 26% [2] and 38% [16]. Since serial sections were done in the current study, the possibility of focal hemosiderin deposits along the vessel length, that could elicit MR changes was excluded. The acute MHs were likely agonal as suggested previously [2]. None of the other studies have characterized MHs as subacute and there seems little justification for characterizing all hemosiderin-positive hemorrhages with edema of the neuropil and lack of

inflammatory changes as chronic [2, 16]. The histology of chronic MHs observed in the current study was similar to previous reports [1, 2, 11].

Although CMBs are generally considered to be markers of focal hemosiderin deposits [1, 11], other vascular pathologies have been observed in the areas of MRI hypointensity. Two hypointensities observed by susceptibility-weighted imaging were found to be due to a dissection in the wall of a grossly distended vessel and in the second case, a microaneurysm was present [2]. The finding that a distended vessel correlates with a hypointensity explains why the three hypointensities (**Table 2**, case 2 #1 and #7, case 3 #2), observed in the current study were related to a single or several large vessel profiles with luminal blood. In a single study of subjects aged 65 and older, hemosiderin deposits which were considered to be the residua of MHs in the putamen, were associated with putaminal microinfarcts suggesting that CMBs detected by MRI may be a surrogate for ischemic pathology rather than exclusively a hemorrhagic diathesis [14]. Supporting these findings is the observation that three of the hypointensities (**Table 2**, case 2 #5 and #10, case 3 #9) observed in this study showed additional microinfarcts by microscopy. In a prior study, a pathologic correlate for 38% of CMBs was not detected [1], while in the present study, no pathologic correlate was found for 13% of CMBs.

Most of the MHs in this study and another large hospital-based autopsy study [27] were located in the white matter or near the grey/white junction where CAA is uncommon, suggesting that CAA may not be an etiological factor in these white matter MHs. Other studies [13, 27, 28] have reported lack of β-amyloid at the site of MHs. However, the findings of focal β-amyloid immunostaining at the bleeding site of one cortical arteriole in the present study, arterioles in a prior study [2] and increased Pittsburg compound B retention at the sites of CAA-related CMBs [29] do not rule out CAA in the etiology of MHs. Possibly, alteration of arteriolar morphology by mural β-amyloid deposition, predisposes to vessel disruption and release of β-amyloid into the bloodstream hence the lack of β-amyloid immunostaining in vessels in remote chronic MHs. This concept explains the presence of β-amyloid upstream or downstream of a bleeding vessel but not at the hemorrhage site [28]. Vascular risk factors such as hypertension are associated with CMBs in otherwise healthy adults [5, 7, 13, 19] and in adults with cerebrovascular diseases [5]. Another vascular risk factor, severe arteriolosclerosis, is reported to correlate with increased numbers of cerebellar MHs [19]. Many of these risk factors were present in the 3 cases in the present study as listed in **Table 1**. Further studies with larger samples are warranted to determine the interplay of the stated factors and possibly additional factors in the pathogenesis of MHs.

CMBs are clinically important in assessing the risk of cognitive impairment and high CMB counts are associated with an increased risk for cognitive deterioration and dementia [30]. Another study while agreeing that CMBs are associated with cognitive impairment in the form of poorer executive function and decline in visuospatial ability, did not observe significant differences in incident dementia rates [31]. In both these studies, CMBs were diagnosed by in vivo MRI only. The limitations of using only in vivo MRI to diagnose CMBs is that MHs of different ages as well as hemorrhagic microinfarcts cannot easily be distinguished. In the present study, ex vivo imaging following by histology facilitated the detection of MHs of different ages and microinfarcts. The limitation of a small sample size in the present study with only 3 cases of Alzheimer's dementia and varying degrees of SVD was offset by neuropathology assessment of 35 CMBs by serial sections and Prussian blue staining for hemosiderin. Hypointensities produced by anatomical landmarks such as the depths of sulci or the entry sites of basal ganglionic vessels can be excluded by making the MRI reader aware of these pitfalls. In summary, in spite of a few limitations, these data suggest that ex vivo imaging is useful to supplement routine neuropathology examination for clinical-pathological correlations in relevant autopsy cases and for research purposes.

Acknowledgements

The authors thank the participants of the Rush Memory and Aging Project and the staff of Rush Alzheimer's Disease Center.

This work was supported by National Institute on Aging grants R01AG064233, R01AG067482, P30AG010161, P30AG072975 and National Disorders and Stroke grants UH2-UH3NS100599 and UF1NS100599.

References

1. Fazekas F, Kleinert R, Roob G, Kleinert G, Kapeller P, Schmidt R, Hartung HP: Histopathologic analysis of foci of signal loss on gradient-echo T2*-weighted MR images in patients with spontaneous intracerebral hemorrhage: evidence of microangiopathy-related microbleeds. AJNR Am J Neuroradiol 1999, 20(4):637-642.
2. Schrag M, McAuley G, Pomakian J, Jiffry A, Tung S, Mueller C, Vinters HV, Haacke EM, Holshouser B, Kido D et al: Correlation of hypointensities in susceptibility-weighted images to tissue histology in dementia patients with cerebral amyloid angiopathy: a postmortem MRI study. Acta Neuropathol 2010, 119(3):291-302.
3. Tanaka A, Ueno Y, Nakayama Y, Takano K, Takebayashi S: Small chronic hemorrhages and ischemic lesions in association with spontaneous intracerebral hematomas. Stroke 1999, 30(8):1637-1642.
4. Koennecke HC: Cerebral microbleeds on MRI: prevalence, associations, and potential clinical implications. Neurology 2006, 66(2):165-171.
5. Cordonnier C, Al-Shahi Salman R, Wardlaw J: Spontaneous brain microbleeds: systematic review, subgroup analyses and standards for study design and reporting. Brain 2007, 130(Pt 8):1988-2003.
6. Vernooij MW, van der Lugt A, Ikram MA, Wielopolski PA, Niessen WJ, Hofman A, Krestin GP, Breteler MM: Prevalence and risk factors of cerebral microbleeds: the Rotterdam Scan Study. Neurology 2008, 70(14):1208-1214.
7. Lu D, Liu J, MacKinnon AD, Tozer DJ, Markus HS: Prevalence and Risk Factors of Cerebral Microbleeds: An Analysis From the UK Biobank. Neurology 2021, 97(15):e1493-e1502.
8. Akoudad S, Portegies ML, Koudstaal PJ, Hofman A, van der Lugt A, Ikram MA, Vernooij MW: Cerebral Microbleeds Are Associated With an Increased Risk of Stroke: The Rotterdam Study. Circulation 2015, 132(6):509-516.
9. Seo SW, Hwa Lee B, Kim EJ, Chin J, Sun Cho Y, Yoon U, Na DL: Clinical significance of microbleeds in subcortical vascular dementia. Stroke 2007, 38(6):1949-1951.
10. De Reuck JL, Cordonnier C, Deramecourt V, Auger F, Durieux N, Bordet R, Maurage CA, Leys D, Pasquier F: Microbleeds in postmortem brains of patients with Alzheimer disease: a T2*-weighted gradient-echo 7.0 T magnetic resonance imaging study. Alzheimer Dis Assoc Disord 2013, 27(2):162-167.
11. Greenberg SM, Vernooij MW, Cordonnier C, Viswanathan A, Al-Shahi Salman R, Warach S, Launer LJ, Van Buchem MA, Breteler MM, Microbleed Study G: Cerebral microbleeds: a guide to detection and interpretation. Lancet Neurol 2009, 8(2):165-174.
12. Kirsch W, McAuley G, Holshouser B, Petersen F, Ayaz M, Vinters HV, Dickson C, Haacke EM, Britt W, 3rd, Larseng J et al: Serial susceptibility weighted MRI measures brain iron and microbleeds in dementia. J Alzheimers Dis 2009, 17(3):599-609.
13. Fisher M, French S, Ji P, Kim RC: Cerebral microbleeds in the elderly: a pathological analysis. Stroke 2010, 41(12):2782-2785.
14. Janaway BM, Simpson JE, Hoggard N, Highley JR, Forster G, Drew D, Gebril OH, Matthews FE, Brayne C, Wharton SB et al: Brain haemosiderin in older people: pathological evidence for an ischaemic origin of magnetic resonance imaging (MRI) microbleeds. Neuropathol Appl Neurobiol 2014, 40(3):258-269.
15. Tatsumi S, Shinohara M, Yamamoto T: Direct comparison of histology of microbleeds with postmortem MR images: a case report. Cerebrovasc Dis 2008, 26(2):142-146.
16. van Veluw SJ, Charidimou A, van der Kouwe AJ, Lauer A, Reijmer YD, Costantino I, Gurol ME, Biessels GJ, Frosch MP, Viswanathan A et al: Microbleed and microinfarct detection in amyloid angiopathy: a high-resolution MRI-histopathology study. Brain 2016, 139(Pt 12):3151-3162.
17. Cordonnier C: Brain microbleeds. Pract Neurol 2010, 10(2):94-100.
18. De Reuck J, Deramecourt V, Cordonnier C, Leys D, Pasquier F, Maurage CA: Prevalence of small cerebral bleeds in patients with a neurodegenerative dementia: a neuropathological study. J Neurol Sci 2011, 300(1-2):63-66.
19. De Reuck JL, Deramecourt V, Auger F, Durieux N, Cordonnier C, Devos D, Defebvre L, Moreau C, Capparos-Lefebvre D, Pasquier F et al: The significance of cortical cerebellar microbleeds and microinfarcts in neurodegenerative and cerebrovascular diseases. A post-mortem 7.0-tesla magnetic resonance study with neuropathological correlates. Cerebrovasc Dis 2015, 39(2):138-143.
20. Nag S, Barnes LL, Yu L, Buchman AS, Bennett DA, Schneider JA, Wilson RS: Association of Lewy Bodies With Age-Related Clinical Characteristics in Black and White Decedents. Neurology 2021, 97(8):e825-e835.
21. Nag S, Yu L, Boyle PA, Leurgans SE, Bennett DA, Schneider JA: TDP-43 pathology in anterior temporal pole cortex in aging and Alzheimer's disease. Acta Neuropathol Commun 2018, 6(1):33.
22. Yu L, Boyle PA, Nag S, Leurgans S, Buchman AS, Wilson RS, Arvanitakis Z, Farfel JM, De Jager PL, Bennett DA et al: APOE and cerebral amyloid angiopathy in community-dwelling older persons. Neurobiol Aging 2015, 36(11):2946-2953.
23. Alemany Ripoll M, Stenborg A, Sonninen P, Terent A, Raininko R: Detection and appearance of intraparenchymal haematomas of the brain at 1.5 T with spin-echo, FLAIR and GE sequences: poor relationship to the age of the haematoma. Neuroradiology 2004, 46(6):435-443.

24. Ahn SJ, Anrather J, Nishimura N, Schaffer CB: Diverse Inflammatory Response After Cerebral Microbleeds Includes Coordinated Microglial Migration and Proliferation. Stroke 2018, 49(7):1719-1726.

25. Jenkins A, Maxwell WL, Graham DI: Experimental intracerebral haematoma in the rat: sequential light microscopical changes. Neuropathol Appl Neurobiol 1989, 15(5):477-486.

26. Koeppen AH, Dickson AC, McEvoy JA: The cellular reactions to experimental intracerebral hemorrhage. J Neurol Sci 1995, 134 Suppl:102-112.

27. Kovari E, Charidimou A, Herrmann FR, Giannakopoulos P, Bouras C, Gold G: No neuropathological evidence for a direct topographical relation between microbleeds and cerebral amyloid angiopathy. Acta Neuropathol Commun 2015, 3:49.

28. van Veluw SJ, Scherlek AA, Freeze WM, Ter Telgte A, van der Kouwe AJ, Bacskai BJ, Frosch MP, Greenberg SM: Different microvascular alterations underlie microbleeds and microinfarcts. Ann Neurol 2019, 86(2):279-292.

29. Dierksen GA, Skehan ME, Khan MA, Jeng J, Nandigam RN, Becker JA, Kumar A, Neal KL, Betensky RA, Frosch MP et al: Spatial relation between microbleeds and amyloid deposits in amyloid angiopathy. Ann Neurol 2010, 68(4):545-548.

30. Akoudad S, Wolters FJ, Viswanathan A, de Bruijn RF, van der Lugt A, Hofman A, Koudstaal PJ, Ikram MA, Vernooij MW: Association of Cerebral Microbleeds With Cognitive Decline and Dementia. JAMA Neurol 2016, 73(8):934-943.

31. Paradise M, Seruga A, Crawford JD, Chaganti J, Thalamuthu A, Kochan NA, Brodaty H, Wen W, Sachdev PS: The relationship of cerebral microbleeds to cognition and incident dementia in non-demented older individuals. Brain Imaging Behav 2019, 13(3):750-761.